1996ApJ...464..622I

THE ASTROPHYSICAL JOURNAL, 464:622–627, 1996 June 20
© 1996. The American Astronomical Society. All rights reserved. Printed in U.S.A.

THE AUTOCORRELATION OF GAMMA-RAY BURST TIME PROFILES

J. J. M. IN 'T ZAND[1] AND E. E. FENIMORE
Los Alamos National Laboratory, Mail Stop D436, Los Alamos, NM 87545
Received 1995 July 7; accepted 1996 January 5

ABSTRACT

The autocorrelation of time profiles of emission from gamma-ray bursts has previously been proved to be a valuable diagnostic for the study of the timing behavior of these bursts. In particular, comparative studies benefited from this diagnostic. However, in these previous studies, the particular shape of the autocorrelation function has not been addressed in great detail. In the present paper we try to explain the autocorrelation shape and behavior. We propose an empirical model that aids in the evaluation of uncertainties in autocorrelation analyses of gamma-ray burst time profiles. Our most important conclusions are that analyses based on the autocorrelation function are not dominated by mathematical properties not connected with the gamma-ray burst phenomenon, and that the uncertainty in the relative time stretching between different photon energy ranges found through such an analysis previously from *CGRO* BATSE data is less than or equal to 10%.

Subject headings: gamma rays: bursts — methods: numerical

1. INTRODUCTION

Correlation functions are frequently used in the analysis of the timing behavior of radiation from stars, usually when the time profile appears to be only noisy to the human eye. These functions are useful to determine typical timescales and correlations in the timing behavior between different times or wavelengths (see, e.g., Sutherland, Weisskopf, & Kahn 1978; Shibazaki et al. 1988). Not only are they useful in the case of apparently noisy data, but also when direct, unbiased investigation of time profiles proves difficult because interesting features have timescales very near to the readout resolution. The latter occurs in gamma-ray burst (GRB) time profiles; a significant amount of the power of the variability occurs near the readout resolution of the Burst and Transient Source Experiment (BATSE) of the *Compton Gamma-Ray Observatory* (*CGRO*). For the most commonly used data format, this resolution is 64 ms.

Here we study the autocorrelation function (ACF) of GRB time profiles. The ACF is defined as follows (Link, Epstein, & Priedhorsky 1993; Fenimore et al. 1995): if the GRB time profile is given by $c_i = m_i - b_i$ counts s^{-1}, where background contributions b_i have been subtracted from the raw count rate m_i, and a time interval of T is selected around the largest peak consisting of N time bins each of duration ΔT s, indexed between $-N/2$ and $+N/2$, the ACF as a function of time lag $j\Delta T$ is

$$A_j = \sum_{i=-N/2}^{N/2} \frac{c_{i+j}c_i}{S} \quad \text{for} \quad j \neq 0 \quad \text{and} \quad A_0 = 1\,, \qquad (1)$$

where the normalization S is

$$S = \sum_{i=-N/2}^{N/2} c_i^2 - m_i\,. \qquad (2)$$

The separate $j = 0$ setting and the $-m_i$ term in S normalizes the ACF so that coherent noise addition at $j = 0$ is eliminated. Thus, it ensures that the expected ACF is count-rate independent. We chose a time interval $T = N\Delta T$ of 16 s (see Fenimore et al. 1995).

Fenimore et al. (1995), following Link et al. (1993), calculated the ACF of GRB time profiles as observed with BATSE with a time resolution of 64 ms as a function of photon energy, averaged over a class of bright GRBs, and determined the typical timescales of the four broad BATSE energy bands using several methods. Irrespective of the method, the energy dependency of the timescale apparently follows a power law with an index of about -0.4. One method involves the calculation of the stretching factor between ACFs of different energy bands. Obviously, this procedure assumes that the ACF is self-similar (i.e., the ACF of a time profile that has been stretched by a factor is equal to the ACF stretched by the same factor). Another method involves the calculation of the full widths at $e^{-0.5}$ of the maximum level. For example, the ACF of channel 1 has a width of 4.3 s. Norris et al. (1995) determined the average shape of single-peak features that can be discerned in time profiles of the same set of GRB BATSE data and found a width for channel 1 of about 0.5 s. This is roughly a factor of 8 smaller than the quoted value for the ACF. However, the energy dependency for the width of the average pulse follows the same power law as the ACF does.

In the present study we try to answer the following questions about the ACF:

1. How accurate is the assumption that GRB time profile ACFs are self-similar?
2. Why is the average ACF so smooth in contrast to ACFs of individual bursts?
3. Why is the typical timescale of the ACF so much larger than expected from time profile studies by Norris et al. (1995), and are these results inconsistent?
4. How valid is the ACF as a tool to determine time stretching, and are there any systematic effects that might mimic time stretching?
5. What is the uncertainty in stretching factors as found from ACFs?

Many GRB time profiles (see, e.g., Fishman et al. 1994) seem to consist of a sequence of shots with a wide range of timescales and shapes. This description is very suggestive of shot noise, as is the exponential behavior of the ACF (Fenimore et al. 1995). Therefore, we use shot noise as a

[1] Present address: NASA/GSFC, Code 661, Greenbelt, MD 2077; jeanz@lhea1.gsfc.nasa.gov.

© American Astronomical Society • Provided by the NASA Astrophysics Data System

1996ApJ...464..622I

base to explain the ACF. In § 2, a general but brief discussion about shot-noise signals and their ACFs is presented. From this, we can understand some of the behavior observed in GRB time profile ACFs. In § 3, a lognormal shot model motivated by the findings of Norris et al. (1996) is introduced in an attempt to complete the explanation of the shape of the GRB time profile ACFs and obtain a method to estimate uncertainties of ACF analyses previously performed. In the conclusion (§ 4), we summarize the answers to the questions posed above.

2. SHOT NOISE

2.1. *The Shot-Noise Signal*

In general, a shot-noise signal is defined by a sum of shots:

$$I(t) = \sum_{i=1}^{\infty} a_i F[t - t_i; c_k(i)] \tag{3}$$

where F is a normalized function of time t (the "shot"), specified by a number of parameters c_k (k between 1 and the number of parameters), values of which are a function of i. The linear combination of many such shots with starting times t_i and amplitudes a_i defines a shot-noise signal if the starting points t_i follow the Poisson distribution for a certain average rate of λ shots per second.

Often, shot-noise models are simplified by assuming that the amplitudes a_i or the shot parameter values c_k are independent of the shot index i. The first assumption helps in dealing with the strong dependence between the amplitude distribution and λ (see § 2.2).

As the term suggests, the shots are often fast-rising functions. Examples of the shot function F are the block function

$$F(t; \tau_F) = \begin{cases} 1 & \text{for } 0 < t < \tau_F \\ 0 & \text{otherwise} \end{cases} ; \tag{4}$$

the exponential function

$$F(t; \tau_F) = \begin{cases} 0 & \text{for } t < 0 \\ e^{-t/\tau_F} & \text{for } t > 0 \end{cases} ; \tag{5}$$

and the two-sided exponential function

$$F(t; \tau_r, \tau_d) = \begin{cases} e^{t/\tau_r} & \text{for } t < 0 \\ e^{-t/\tau_d} & \text{for } t > 0 \end{cases} . \tag{6}$$

More complex shot-noise signals involve values for a_i and $c_k(i)$, which are sampled from distributions or follow a certain time-dependent function.

Norris et al. (1994, 1995) investigated GRB time profiles by searching for structure in the time profiles themselves. They found that many time profiles can be described as a sum of "pulses," where the pulses are given by

$$F(t; \tau_r, \tau_d, \nu) = \begin{cases} e^{-(|t|/\tau_r)^\nu} & \text{for } t < 0 \\ e^{-(|t|/\tau_d)^\nu} & \text{for } t > 0 \end{cases} , \tag{7}$$

which is identical to equation (6) except for the "peakedness" parameter ν. The parameters τ_r, τ_d, and ν are free parameters found by optimizing a goodness of fit.

2.2. *The ACF of Shot Noise*

Rice (1954) derives a general expression for the expected autocorrelation function of shot noise, assuming equally sized shots ($a_i = 1$ for all i) and an infinite time series:

$$\bar{A}(\tau) = \lambda \int_{-\infty}^{\infty} F(t; c_k) F(t + \tau; c_k) dt + \left[\lambda \int_{-\infty}^{\infty} F(t; c_k) dt \right]^2 , \tag{8}$$

where τ is the time lag. If we sample any arbitrary time interval of length T out of this infinite series and normalize the ACF so it conforms to equation (1), the resulting ACF averaged over many samples is expected to be

$$\bar{A}_N(\tau) = \frac{\bar{A}(\tau)}{\bar{A}(\tau = 0)} \left(1 - \frac{|\tau|}{T} \right) . \tag{9}$$

For the three simple shot-noise models above (eqs. [4]–[6]) and if $\tau_w \equiv \lambda^{-1}$ (average wait time between two subsequent shots) this becomes

1. If the shots are modeled by equation (4),

$$\bar{A}_N(\tau) = \left[\alpha \left(1 - \frac{|\tau|}{\tau_F} \right) + (1 - \alpha) \right] \left(1 - \frac{|\tau|}{T} \right) , \tag{10}$$

with $\alpha = \tau_w/(\tau_w + \tau_F)$.

2. If the shots are modeled by equation (5),

$$\bar{A}_N(\tau) = [\alpha e^{-|\tau|/\tau_F} + (1 - \alpha)] \left(1 - \frac{|\tau|}{T} \right) , \tag{11}$$

with $\alpha = \tau_w/(\tau_w + 2\tau_F)$.

3. If the shots are modeled by equation (6),

$$\bar{A}_N(\tau) = \left[\alpha \frac{\tau_d e^{-|\tau|/\tau_d} - \tau_r e^{-|\tau|/\tau_r}}{\tau_d - \tau_r} + (1 - \alpha) \right] \left(1 - \frac{|\tau|}{T} \right) , \tag{12}$$

with $\alpha = \tau_w/[\tau_w + 2(\tau_r + \tau_d)]$.

Each of these expressions contains three items: a term based on the shot function, a constant term $1 - \alpha$, and a triangular envelope factor $1 - |\tau|/T$. The constant term can be imagined as a background level that is caused by overlapping shots. This background can dominate the signature of all shots in the ACF if there is extensive overlap, indicated by a small value for α (which is a monotonic function of the ratio between wait time and shot width).

We were unsuccessful in deriving analytical expressions for the ACFs of more complicated shot-noise signals (like ones that mimic GRB time profiles, as described by eq. [7]). Therefore, these were calculated numerically instead by averaging the ACFs over a sufficient number of realizations of all parameters. It can be expected that the response of the ACF to the limited time interval T and to the overlap between shots will be similar to the ACF for the simple examples above, while the exact dependence of parameters might differ.

To some extent, the ACF averages the time profile. Therefore, not surprisingly, the ACF prohibits a detailed simultaneous analysis of many parameters. To determine meaningful values for a few parameters, it often makes sense to adopt values for the other ones from an independent source.

Sometimes, there is a strong dependency between different parameters in the ACF. A good example of this is the following. The ACF of a shot-noise signal consisting of a sequence of single-sided exponential shots, with a mean

© American Astronomical Society • Provided by the NASA Astrophysics Data System

1996ApJ...464..622I

wait time of τ_w and an exponential distribution for the amplitude, is identical to the ACF of a sequence of such shots with a mean wait time of $2\tau_w$ and a constant amplitude. This equivalence may be readily derived from an equation similar to equation (8), but which includes a distribution for the amplitude,

$$\bar{A}(\tau) = \left[\int_{a=0}^{\infty} p(a)a^2 da\right]\lambda\int_{-\infty}^{\infty} F(t; c_k)F(t+\tau; c_k)dt + \left\{\int_{a=0}^{\infty} a\left[\int_{x=0}^{\infty} \frac{p(x)p(a/x)}{x}\,dx\right]da\right\} \times \left[\lambda\int_{-\infty}^{\infty} F(t; c_k)dt\right]^2, \quad (13)$$

where a is the amplitude and $p(a)$ is the probability for an amplitude between a and $a + da$. For an exponential amplitude distribution and a shot function according to equation (5), working out equation (9) with equation (13) substituted reveals

$$\bar{A}_N(\tau) = [\alpha e^{-|\tau|/\tau_F} + (1-\alpha)](1 - |\tau|/T), \quad (14)$$

with $\alpha = \tau_w/(\tau_w + \tau_F)$. Equation (14) is identical to equation (11) except for an increase in τ_w by a factor of 2.

To obtain a sense of what characteristics of the GRB time profile are important to the ACF, we performed a number of simulations. Typically, 1000 simulations were performed for one set of parameter distributions to obtain a well-defined average of the ACF. One set of the simulations involved changing the distributions of c_k while preserving the average values; we find that does not change the ACF drastically. However, changing the distribution for the wait times from a Poissonian one-to-one with a lower cutoff strongly affects the ACF. The reason for this sensitivity is clear from the implications for the time profiles. If a distribution has a cutoff at small wait times, the probability for two or more shots being right on top of each other is less than in the Poisson case, particularly if the cutoff is at a wait time larger than the mean shot width. If this cutoff is large, while the mean wait time stays the same, the background level introduced by overlap of shots is smaller, and, thus, the ACF signal of the shots will be stronger.

In Figure 1, three examples of ACFs are plotted, two of which are for shot-noise signals. From these examples a few characteristics of the ACF are immediately obvious. First, the ACF of a shot-noise signal is broader than that of a single shot with a width equal to that of the average shot in the shot-noise signal. This is mainly owing to the statistics of many shots; for relatively small wait times these tend to cluster and thus can be thought of as combined shots that are wider. Second, the ACF is *not* a self-similar function in the sense that stretching the shots with a constant factor implies that the ACF is stretched by the same factor for every time lag. This is also mathematically clear in the case of classical shot noise from equation (8), where the second term (representing overlap of shots and having no dependence on lag) makes the ACF non–self-similar. Therefore, even if the ACF of a single shot is self-similar, the ACF of a series of shots is not. However, ACFs are approximately self-similar up to a certain lag, the value of which is larger when the overlap between shots is smaller (i.e., when α is larger). Third, different models of time profiles can result in very similar normalized ACFs. Thus, the ACF is not a very sensitive tool to discriminate between different models of time profiles. Conversely, our use of a simple model to mimic GRB time profiles is justified.

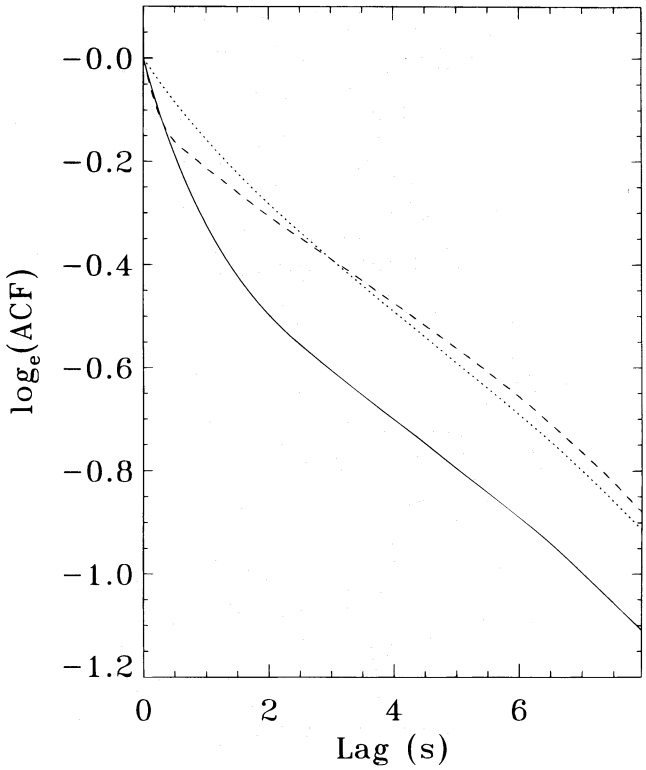

FIG. 1.—Examples of ACFs of shot noise with a single-sided exponential shot of decay time 1 s (*solid curve*) and 2 s (*dotted curve*). In both cases, the average wait time is 1 s with a Poisson distribution. The dashed curve is for the same signal as the solid curve except for a lognormal distribution for the wait times with a logarithmic standard deviation of 0.2. Apparently, the ACF of shot noise is not self-similar, and observed ACFs can easily be modeled by different models.

3. A LOGNORMAL SHOT MODEL FOR THE ACFS OF BATSE GRB TIME PROFILES

We have constructed a model for the time profiles of GRBs that is motivated by the results obtained by Norris et al. (1996), from an analysis of pulses[2] in a set of GRB time profiles observed with BATSE. The purpose of this model is twofold: first, to check whether the ACFs are consistent with the results by Norris et al. regarding the widths of the shots, and, second, to determine statistical uncertainties of the ACF analysis performed by Fenimore et al. (1995).

3.1. *Model Description*

The model is derived from the shot-noise model. However, the key difference from shot noise is an asymmetrical lognormal (see below for an explanation) instead of exponential (or Poissonian) distribution of wait times between shots. We will refer to this model as the lognormal shot model. The shots are described by equation (7), except that they will be parameterized by the full width at half-maximum (FWHM), f, and the rise-to-decay ratio instead of

[2] Here we stress the difference between *shots* and *pulses*: shots are the features that are part of shot-noise or lognormal shot models, pulses are the features observed in gamma-ray time profiles. We purely compare statistical properties of these.

© American Astronomical Society • Provided by the NASA Astrophysics Data System

1996ApJ...464..622I

τ_r and τ_d. Because of the relationship $\tau_r = 0.33\tau_d^{0.83}$ as found by Norris et al. (1996), the rise-to-decay ratio is a function of f and will not be a free parameter of our lognormal shot model (we note that the ACF is only marginally sensitive to the relation between τ_r and τ_d). The FWHM f, the peakedness v, and the shot amplitude a are sampled from lognormal distributions.

A lognormal distribution is defined by a Gaussian function in the logarithmic domain and is described by two parameters: the average of the logarithms of the parameter values $\langle \log_{10} p \rangle$ and the standard deviation σ. We note that the relationship between logarithmic and linear average $\langle p \rangle$ is given by

$$\langle p \rangle = 10^{\langle \log_{10} p \rangle} \times 10^{\sigma_{10}^2/2 \log_{10} e}, \quad (15)$$

where σ_{10} is the standard deviation in $\log_{10} a$. In an asymmetric lognormal distribution, the left- and right-sided branches of the Gaussian function have different standard deviations.

The lognormal shot model has eight parameters: $\langle f \rangle$, σ_f, $\langle \tau_w \rangle$, $\sigma_{\log_{10} \tau_w}$ (*left*), $\sigma_{\log_{10} \tau_w}$ (*right*), $\langle v \rangle$, $\sigma_{\log_{10} v}$, and σ_a/a. The absolute values of the amplitudes are not relevant if one analyzes normalized ACFs. For four BATSE energy channels, the total number of parameters increases to 11 if only f is dependent on energy. We assume here that there is a one-to-one mapping of shots between different energy bands and that wait times are identical in all bands, and we notice that when one compares ACFs from different groups of bursts, this assumption might not apply (for instance, in a cosmological scenario for GRBs, the average wait time might be a function of brightness because of the presence of time dilation due to the expansion of the universe). The photon energy ranges for the four BATSE channels are as follows: 25–57 keV (channel 1), 57–115 keV (channel 2), 115–320 keV (channel 3), and 320–1000 keV (channel 4).

3.2. *The Average Shot FWHM As Found from the ACF*

We are interested in the widths of the average shots that result from applying the lognormal shot model, in order to check whether these are consistent with the widths of the average separable pulses found by Norris et al. (1996). The values for the other parameters were adopted from the distributions published in Norris et al. The values of the fixed parameters thus obtained are $\sigma_f = 0.26$, $\langle \tau_w \rangle = 0.6$ s, $\sigma_{\log_{10} \tau_w}$ (*left*) = 0.3, $\sigma_{\log_{10} \tau_w}$ (*right*) = 0.6, $\sigma_{\log_{10} v} = 0.13$, and $\sigma_a/a = 0$ (the shot amplitude is assumed constant). We found that we needed to treat the peakedness $\langle v \rangle$ also as a free parameter in order to get good fits between model and observed ACFs. The best value for $\langle v \rangle$ is 0.8. The best-fit values for the FWHMs are $\langle f \rangle_1 = 0.60$ (0.66), $\langle f \rangle_2 = 0.46$ (0.49), $\langle f \rangle_3 = 0.33$ (0.39), and $\langle f \rangle_4 = 0.22$ s (0.26) (the values found by Norris et al. 1996 are given in parentheses). Figure 2 presents a graphical comparison between fits and data. This result shows that the observed ACFs are indeed consistent with the results on pulses in GRB time profiles as found by Norris et al.

3.3. *Uncertainties in ACF Analysis*

There are two sources of uncertainty in the ACF analysis. First, there is that uncertainty due to photon counting statistics. In Figure 3, we show the spread that is expected in the ACF due to photon counting statistics. This is a simu-

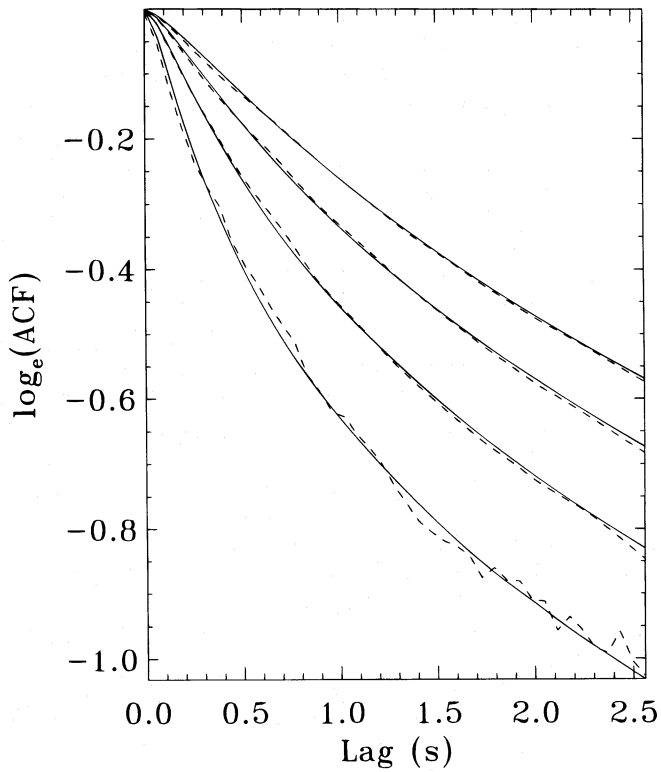

FIG. 2.—Fits of the lognormal shot model (*solid lines*) to BATSE ACFs (*dashed lines*), for four energy channels (the width decreases with the energy) and for the first 2.5 s of lag. The model is a satisfactory representation of the ACF of GRB time profiles and is in agreement with findings by Norris et al. (1995).

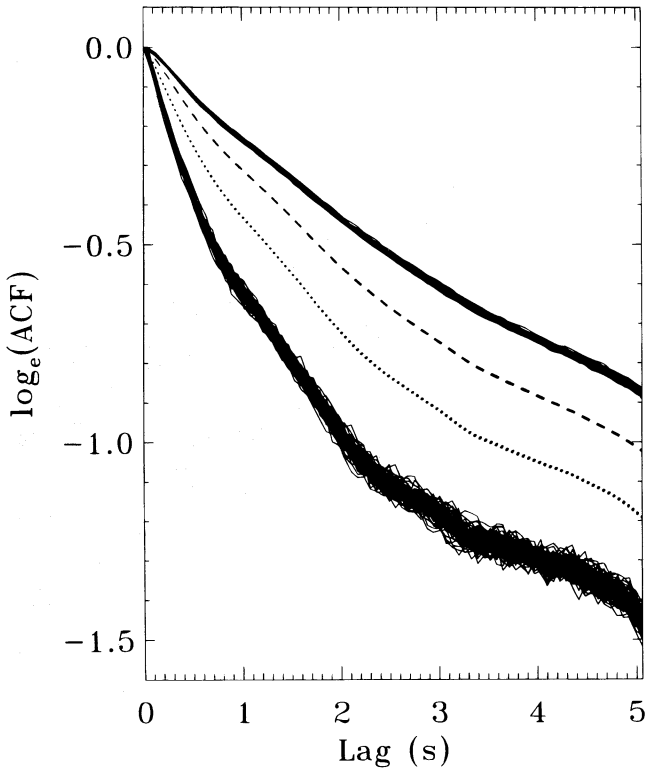

FIG. 3.—Expected spread in the BATSE ACFs as a result of photon count statistics for the lognormal shot model for energy channels 1 (*upper set of solid curves*), 2 (*dashed*), 3 (*dotted*), and 4 (*lower solid curves*). Channels 2 and 3 have a spread about the thickness of the lines. The Poisson variations in channels 1 and 4 are small, so that the overall effect of the Poisson noise is small.

© American Astronomical Society • Provided by the NASA Astrophysics Data System

1996ApJ...464..622I

lated result: we calculated time profiles of a sample of 41 bursts from the above lognormal shot model (with a different FWHM for the four BATSE channels), multiplied these with the average peak count rates in the four BATSE channels, added average background levels as expected in these channels, randomly sampled the count rates from a Poisson distribution, calculated the ACFs and averaged the results over the 41 bursts, and repeated this procedure 100 times, changing only the seed value of the random sampling of count rates. As can be derived from this figure, the accuracy of the BATSE measurements is quite good in this domain.

The second source of uncertainty is the fact that we only observed 41 bursts with shots from three very wide distributions out of the lognormal shot model. Obviously, this number is quite small, and the resulting spread in the ACF is expected to be relatively large (see Fig. 4). The spread is largely due to the wide distribution of wait times. The spread due to the distribution of FWHMs is at least a factor of 5 smaller than this. This is an important fact because this means that for the same 41 BATSE bursts the relative accuracies between the four energy bands is quite good (i.e., if we assume that the sequence of wait times is the same for all four bands). If S_{i1} is the stretching factor from BATSE energy channel i to channel 1, the complete result for the three stretching factors is (combining the factors found by Fenimore et al. 1995 and the rms values found here) $S_{21}^{-1} = 0.78 \pm 0.02$, $S_{31}^{-1} = 0.54 \pm 0.02$, and $S_{41}^{-1} = 0.33 \pm 0.02$. The results for the widths of the ACFs at $e^{-0.5}$ times the maximum are $W_{ac(1)} = 4.3 \pm 0.50$ s, $W_{ac(2)} = 3.4 \pm 0.4$ s, $W_{ac(3)} = 2.3 \pm 0.3$ s, and $W_{ac(4)} = 1.5 \pm 0.2$ s.

When one assumes that the ACFs are self-similar, one will make a systematic error in relating stretching factors to ratios of shot FWHMs. If one uses the ACF within 2.5 s of the maximum (as did Fenimore et al. 1995), the lognormal shot model indicates that, going from BATSE channel 4 to channel 1, the ACF will be stretched by 10% less than are the shots. This percentage is lower for stretching between other channels. The identification of the data with a power-law model is, therefore, not noticeably affected. This systematic error indicates that the power-law index in the shot width versus photon energy relationship is about 10% steeper than that in the ACF width versus energy, as reported by Fenimore et al. (1995). The 10% number is not significant since it is of the same order as the statistical rms error for 41 bursts.

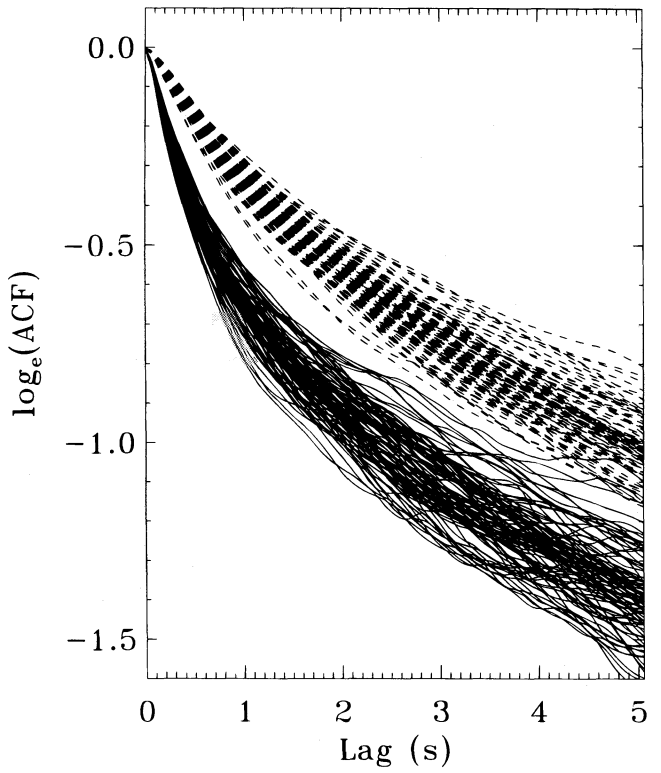

FIG. 4.—Expected spread in the BATSE ACFs due to sampling from the three distributions in the lognormal shot model, for energy channels 2 (*dashed curves*) and 4 (*solid curves*). Although the spread is wide, this does not affect the measurement of the shot width dependence on energy as much in this model, since the ACFs in all channels either all get narrower or all get wider. The stretching between ACFs in different channels is nearly constant (see text).

4. CONCLUSIONS

We have studied a number of questions with respect to the average ACF of a set of GRBs observed with BATSE, and we conclude the following:

1. Although the ACF is formally *not* a self-similar function, the systematic error in the stretching factor between the average ACFs of different energy channels for the bright BATSE bursts when assuming self-similarity is $\leq 10\%$ for the first 2.5 s lag.
2. The average ACF is smooth because one averages over many shots within bursts, rather than over a few GRBs.
3. Although the ACF, at first glance, suggests timescales much larger than found from analyses of individual shots, a more detailed look at the ACF shape shows that both diagnostics are consistent in terms of average shot widths and wait times between shots.
4. There are no systematic effects that can mimic time stretching in an ACF.
5. The rms errors in the stretching factors as determined by Fenimore et al. (1995) are 0.02, which is equivalent to the systematic error (point 1 above).

The ACF can teach us similar GRB characteristics as direct studies of GRB time profiles can. Although an ACF analysis is much more restrictive, it is less prone to selection effects and, thus, can be of some supplemental value.

We have used the concept of shot noise in the study of GRB ACFs, partly because these ACFs are quite suggestive of shot noise. However, this does not mean the time profiles actually are shot noise. We needed to incorporate a lognormal distribution for the wait time to obtain a more complete empirical description of time profiles and way of explaining more than just the ACF. Thus, we left the classical concept of shot noise. One should be very cautious in making statements about time profiles from the ACF alone. A statement from an analysis of several KONUS/*Venera* observed GRBs (Belli 1992) in the power spectrum domain (similar to the ACF domain), saying that their time profile can be interpreted as a shot-noise process, seems premature.

This work was done under the auspices of the US Department of Energy and was funded in part by the *Compton Gamma Ray Observatory* Guest Investigator program.

© American Astronomical Society • Provided by the NASA Astrophysics Data System

1996ApJ...464..622I

REFERENCES

Belli, B. M. 1992, ApJ, 393, 266
Fenimore, E. E., In 't Zand, J. J. M., Norris, J. P., Bonnell, J. T., & Nemiroff, R. J. 1995, ApJ, 448, L101
Fishman, G. J., et al. 1994, ApJS, 92, 229 (first BATSE GRB catalog)
Link, B., Epstein, R. I., & Priedhorsky, W. C. 1993, ApJ, 408, L81
Norris, J. P., Nemiroff, R. J., Bonnell, J. T., Scargle, J. D., Kouveliotou, C., Paciesas, W. S., Meegan, C. A., & Fishman, G. J. 1996, ApJ, 459, 393
Norris, J. P., Nemiroff, R. J., Scargle, J. D., Kouveliotou, C., Fishman, G. J., Meegan, C. A., Paciesas, W. S., & Bonnell, J. T. 1994, ApJ, 424, 540
Rice, S. O. 1954, in Selected Papers on Noise and Stochastic Processes, ed. N. Wax (New York: Dover), 133
Shibazaki, N., Elsner, R. F., Bussard, R. W., Ebisuzaki, T., & Weisskopf, M. C. 1988, ApJ, 331, 247
Sutherland, P. G., Weisskopf, M. C., & Kahn, S. M. 1978, ApJ, 219, 1029

© American Astronomical Society • Provided by the NASA Astrophysics Data System